**ATF2 contributes to cisplatin resistance in non-small cell lung cancer and celastrol induces cisplatin resensitization through inhibition of JNK/ATF2 pathway.**

# ATF2 contributes to cisplatin resistance in non-small cell lung cancer and celastrol induces cisplatin resensitization through inhibition of JNK/ATF2 pathway

**Int J Cancer. 2015 Jun 1;136(11):2598-609. doi: 10.1002/ijc.29302**

**Authors: Lo Iacono M[1], Monica V, Vavalà T, Gisabella M, Saviozzi S, Bracco E, Novello S, Papotti M, Scagliotti GV.**

**ATF2 contributes to cisplatin resistance in non-small cell lung cancer and celastrol induces cisplatin resensitization through inhibition of JNK/ATF2 pathway**

Authors: Lo Iacono M[1], Monica V, Vavalà T, Gisabella M, Saviozzi S, Bracco E, Novello S, Papotti M, Scagliotti GV.

## Abstract

ATF2 is a transcription factor involved in stress and DNA damage. A correlation between ATF2 JNK-mediated activation and resistance to damaging agents has already been reported. The purpose of the present study was to investigate whether ATF2 may have a role in acquired resistance to cisplatin in non-small cell lung cancer (NSCLC). mRNA and protein analysis on matched cancer and corresponding normal tissues from surgically resected NSCLC have been performed. Furthermore, in NSCLC cell lines, *ATF2* expression levels were evaluated and correlated to platinum (CDDP) resistance. Celastrol-mediated ATF2/cJUN activity was measured. High expression levels of both *ATF2* transcript and proteins were observed in lung cancer specimens ($p << 0.01$, $Log_2(FC) = +4.7$). CDDP-resistant NSCLC cell lines expressed high levels of ATF2 protein. By contrast, Celastrol-mediated ATF2/cJUN functional inhibition restored the response to CDDP. Moreover, ATF2 protein activation correlates with worse outcome in advanced CDDP-treated patients. For the first time, it has been shown NSCLC ATF2 upregulation at both mRNA/protein levels in NSCLC. In addition, we reported that in NSCLC cell lines a correlation between ATF2 protein expression and CDDP resistance occurs. Altogether, our results indicate a potential increase in CDDP sensitivity, on Celastrol-mediated ATF2/cJUN inhibition. These data suggest a possible involvement of ATF2 in NSCLC CDDP-resistance.



Non-small cell lung cancer (NSCLC) is characterized by high incidence and mortality rate worldwide, being the most common subtypes represented by adenocarcinoma and squamous cell carcinoma.[1] Platinum-based chemotherapy in combination with other cytotoxic agents such as Gemcitabine, taxanes and vinorelbine represented the standard of care for unselected patients with advanced NSCLC. Recently, in nonsquamous histology, the combination of cisplatin (CDDP) and pemetrexed showed superior activity.[2, 3] However, in chemotherapy-treated NSCLC, the duration of response is relatively short due to primary or acquired resistance to chemotherapy.[4] Patients with advanced disease may not derive any benefit from first-line chemotherapy, while they face significant treatment-related side effects. Consequently, it appears a logical approach to investigate alternative ways to increase the effectiveness outcomes of chemotherapy, through the identification of molecular features suggestive of a better therapeutic ratio.

Activating transcription factor 2 (ATF2) is a member of the basic helix-loop-helix (b-ZIP) transcription factor family, whose transcriptional activities are mediated by stress-activated kinases JNK/p38 and activated by phosphorylation on threonine residues.[5, 6] Independent of its transcriptional activity, ATF2 also plays an important role in the DNA damage response and in the regulation of intra-S-phase checkpoint (reviewed in Ref. [7]). Several studies reported a correlation between ATF2/JNK-mediated activation and resistance to DNA damaging agents. Hayakawa *et al*. showed that stable expression of *ATF2* in human breast carcinoma cells BT474 conferring resistance to DNA-damaging agents, secondary to an increased DNA repair ability and this status may be reverted by blocking ATF2 activation using JNK inhibitor (SP600125).[8] Furthermore, cJUN/ATF2 complex play a role in cell transformation by inducing anchorage and/or growth factor-independent proliferation.[9] Similar findings were also reported in melanoma and, in this type of tumor, ATF2 nuclear localization is associated with poor prognosis.[10]

Celastrol, a triterpene known as tripterine, is an ingredient extracted from a plant and traditional Chinese medicine uses it as an anti-inflammatory agent. It is active against rheumatoid arthritis,[11]

allergic asthma[12] and systemic lupus erythematosus.[13] In several cancer models, both *in vitro* and *in vivo*, Celastrol showed promising anticancer activity. It induces apoptosis in different cancer cells[14-19] and inhibits the growth of glioma, melanoma and prostate cancer in nude mice.[15, 20, 21] In addition, it synergistically enhances the cytotoxicity of ionizing radiation, gambogic acid, TRAIL/APO-2L and temozolomide.[22-24] Although several hypothetical cellular targets for celastrol have been reported, its mechanism of action has not been fully elucidated. Celastrol affects several biological processes through the inhibition of ATF2, nuclear factor-KB, inducible NOS, VEGF receptors, HSP90, potassium/calcium channel and eventually increases the reactive oxygen species (ROS) in cancer cells, thus in turn activating apoptosis pathways.[16, 22, 25-29]

In the present study, we investigated whether *ATF2* could contribute to primary and/or acquired drug resistance in NSCLC. We demonstrated that high expression levels of *ATF2*, at transcript and protein levels, are detected in NSCLC and ATF2 protein activation correlates with worse outcome in advanced NSCLC patients cisplatin-treated. In addition, cisplatin-resistant NSCLC cell lines expressed high levels of ATF2 protein and functional inhibition of ATF2/cJUN by celastrol restored the sensitivity to cisplatin.

## Material and Methods

### Cell culture conditions

NSCLC cell lines were purchased at American Type Culture Collection (ATCC) and were all grown in RPMI (Gibco: Thermo Fisher Scientific, Waltham, MA) medium supplemented with 10% fetal bovine serum (FBS) supplemented with penicillin/streptomycin and maintained at 37°C with 5% $CO_2$.

### Protein extracts and immunoblotting

To isolate total protein content, cells were lysed on ice with RIPA buffer [50 mM Tris-HCl (pH 8.0), 150 mM NaCl, 1% Triton X-100, 0.1% SDS, 0.5% sodium deoxycholate and freshly added of 2 mM sodium orthovanadate, protease and phosphatase inhibitors cocktails (Sigma, St Louis, MO)], and cell debris removed by centrifugation at 16000 RCF at 4°C for 10 min.

The nuclear proteins isolation was performed as follows: cells were lysed in cytoplasmic lysis buffer (10 mM HEPES, 10 mM KCl, 0.1 mM EDTA, 0.625% NP40) for 30 min on ice. Subsequently, lysates were collected and centrifuged at 16000 RCF for 1 min. The pellet containing nuclei was resuspended in nuclear lysis buffer (20 mM HEPES, 0.42 M NaCl, 5 mM EDTA, 10% glycerol) and incubated on a rotary shaker for 30 min at 4°C. Nuclear debris were spinned-down and discarded by a centrifugation step at 16000 RCF for 10 min at 4°C.

Proteins dephosphorylation by Calf Intestine Alkaline Phosphatase (CIAP): 10 μg of CDDP treated total lysate were incubated for 3 hr in CIAP buffer (1x) with or without 10 Units of CIAP enzyme (Promega, Madison, WI). Evaluation of cJUN was performed by Western Blot analysis.

Equal amounts of protein (35 μg/well) for each sample were loaded and analyzed through SDS-PAGE. Proteins were then transferred onto PVDF membranes (Immobilon P-, Millipore, Billerica, MA), blocked in 5% nonfatty acid milk for at least 1 hr and incubated overnight at 4°C with the primary antibodies (1:1000 dilution) against phospho-specific ATF2 (F-1) (sc-8398), ATF2 (N-96) (sc-6233), c-Jun (H-79) (sc-1694), phospho-specific-Jun (sc822; Santa Cruz Biotechnology, Heidelberg, Germany). The signal was visualized by chemiluminescence reagents (Super Signal West Pico kit; Pierce: Thermo Fisher Scientific).

### Flow cytometry ATF2 and phospho-ATF2 protein expression measurements

$2\times10^5$ cells from 2 different lung cancer cell lines (H522, H1395) were incubated for 6 hr with cisplatin (CDDP) doses ranging between 0 and 200 µM (CDDP). The cells were then washed with PBS + 0.1% EDTA for 5 min at 37°C, detached and subsequently pelleted by centrifugation for 1 min at 1500 RCF 4°C. The resulting pellet was resuspended in the residual PBS plus 1 ml of glacial cold (−20°C) methanol and incubated for 10 min at −20°C. Cells were subsequently washed twice with PBS + 1% BSA and permeabilized with PBS + 1% BSA + 0.1% TRITON-x100 for 15 min in the dark. Following these cells were stained with primary antibodies (ATF2 or pATF2) diluted 1:100 in PBS + 1% BSA + 0.1% TRITON-x100 for 30 min at room temperature. Cells were than washed twice with PBS and then stained with secondary antibody fluorescently conjugated with alexa488 (1:1000; Invitrogen: Thermo Fisher Scientific) for 30 min at room temperature, washed again twice with PBS and analyzed by FACS CyAN adp (Beckman & Coulter, Brea, CA).

**Immunofluorescence**

$2\times10^4$ cells from 2 different lung cancer cell lines (H522, H1395), previously seeded onto cover slips, were incubated for 6 hr with CDDP doses ranging between 0 and 200 µM. Afterwards, cells were washed with PBS and incubated in glacial cold methanol (−20°) for 5 min at RT. Subsequently, cells were blocked with PBS + 1% FBS for 30 min at RT and then incubated with the primary antibodies against ATF2 or pATF2 (diluted 1:100 in PBS + 1% FBS) for 1 hr at 37°C. Finally, cells were stained for 1 hr at 37°C with a secondary antibody alexa488 conjugated (diluted 1:1000). Propidium iodide staining for 5 min at room temperature visualized nuclei. The slides were then mounted and analyzed by ZEISS Microscope.

**Cell lines treatment, transfection and viability evaluation**

To evaluate the ability of different drugs (CDDP, JNK inhibitors SP600125, Celastrol and Celecoxib) to modulate ATF2-mediated gene expression, we engineered the pGL3 plasmid with the 8xATF2 Response Elements extracted from ATF2 decoy plasmid kindly provided by Prof. Mingtao Li.[30]

One day prior to transfection, H522 cells ($2 \times 10^5$ cells/well) were seeded into a 6-well tissue culture plate and cultured with 2 mL fresh complete RPMI-1640 medium. Cells were then transfected with lipofectamine 2000 (Invitrogen) using 1 µg of 8xATF2-pGL3 per well according to manufacturer's instructions. After transfection, cells were cultured for two days or incubated with drugs as detailed in Fig. 3. After incubation with drugs, cells were lysed by Passive Lysis Buffer (Promega, Madison, WI) and luminescence measured by luminometer (Victor Light 1420; Perkin Elmer, Waltham, MA).

The 3-(4,5-dimethylthiazol-2-yl)-5-(3-carboxymethoxyphenyl)-2-(4-sulfophenyl)−2Htetrazolium (MTS) viability assay was performed as follows: cells were cultured for 24 hr testing different drug concentrations (Celastrol: 0–5 µM, Cisplatin: 0–300 µM); for each drug, the range of increasing concentrations was selected to maximize the sigmoidal pattern of dose-response graph. To outline a variation in the dose-response graph, drugs combination effect was tested by mixing the doses used for each single treatment (Mix.1= DrugA.[1]+DrugB.[1] … Mix.8= DrugA.[8]+DrugB.[8]). Briefly, MTS was added according to manufacturer's instructions (Promega) and after 1–2 hr of incubation at 37°C, the absorbance at 490 nm was recorded by ELISA reader. Technical quadruplicates were performed for each drug conditions and the experiment was replicated at least 2 times. The half maximal inhibitory concentration at 24h ($IC50_{24}$) is a measure of the effectiveness of a molecule/drug inhibiting a specific biological or biochemical function. In our analysis, this is the concentration of a single drug, or combinations of drugs, endowing viability reduction of 50% after 24h of drug exposure. $IC50_{24}$ values were calculated by evaluating the viability data with Sigmoidal Dose Response analysis using GraphPad software and Combination Index (CI) calculated using mutually non-exclusive formula:

$$D1/Df1 + D2/Df2 + (D1\ D2)/(Df1\ Df2)$$

where D1 and D2 are the concentrations of the combination required to produce survival *f* (50% in our study); D*f*1 and D*f*2 are the concentrations of the component drugs required to produce f. For the analysis, synergy was defined when CI values < 1.0, antagonism when CI values > 1.0 and additivity CI values equal to 1.0. To simplify the results interpretation decimal CI values were expressed as "percentage of effect" in text (i.e. CI 0.25 = effect increased by 75% -synergy- or CI 1.5 = effect decreased by 50% -antagonism-).

**RNA extraction, cDNA synthesis and qPCR**

Total RNA was extracted either from cell lines or from 60–80 mg of tumor and normal lung tissue specimens. Genomic DNA contamination was removed by DNAseI treatment (Promega). RNA was then quantified via Nanodrop (Thermo Fisher Scientific) and stored at −80°C. Two μg total RNA were retro-transcribed with random hexamer primers and Multiscribe Reverse transcriptase (High Capacity cDNA Archive Kit, Applied Biosystems: Thermo Fisher Scientific), according to manufacturer's instructions. Expression levels of *ATF2*, *cJUN* and reference *UBC* genes were evaluated with SYBR technology with optimized PCR conditions and primer concentrations. Primer sequences were as follows:

ATF2.fw: 5′-TACAAGTGGTCGTCGG-3′; ATF2.rv: 5′-CGGTTACAGGGCAATC-3′; UBC.fw: 5′-GTCGCAGTTCTTGTTTGTGGATC-3′; UBC.rv: 5′-GTCTTACCAGTCAGAGTCTTCACGAAG-3′; cJUN.fw: 5′-CGGAGAGGAAGCGCATGA-3′; cJUN.rv: 5′-TTCCTTTTTCGGCACTTGGA-3′.

Melting curve analyses and efficiency evaluation were performed for all the amplicons. Quantitative PCR (qPCR) was carried-out on an ABI PRISM 7900HT Sequence Detection System (Applied Biosystems) in 384-well plates assembled by Biorobot 8000 (Qiagen, Germantown, ML). Reactions were performed in a final volume of 20 μl. All qPCR mixtures contained 1 μl of cDNA template, 1X SYBR Universal PCR Master Mix (Applied Biosystems). Amplification conditions were conducted as follows: after an initial 2 min hold at 50°C to allow AmpErase-UNG activity and 10 min at 95°C, the samples were cycled 40 times at 95°C for 15 sec and 60°C for 1 min. Baseline and threshold for Ct calculation was setup manually with the ABI Prism SDS 2.1 software.

**Patients and samples**

**ATF2 mRNA analysis population**

Frozen primary lung tumors and paired corresponding non-neoplastic lung specimens of 86 consecutive NSCLC patients who underwent radical surgery were collected from the Division of Thoracic Surgery at the San Luigi Hospital between December 2003 and March 2005.

Patients (67 males and 19 females) had a median age of 67 years (range 40 to 82 years) and none of them received either preoperative or postoperative chemo and/or radiotherapy, according to the institutional treatment policy for resectable rescue in those years. Histological examination was performed on formalin-fixed paraffin-embedded tissues in all cases and tumors were diagnosed and classified according to the WHO classification,[31] as follows: 41 adenocarcinoma (ADC); 32 squamous cell carcinoma (SQC); 5 large cell carcinoma (LCC); and 8 bronchiolo-alveolar carcinoma/adenocarcinoma in situ (BAC/AIS). Differentiation grade (grade 1: 17, grade 2: 29, grade 3: 40), pT status (pT1: 9, pT2: 58, pT3: 10, pT4: 9) and pN status (pN0: 53, pN1: 16, pN2: 17) were also recorded. According to the TNM classification for solid tumors WHO 2004,[31] 40 cases were pathological stage I, 19 stage II, 24 stage III and 3 stage IV. Follow up data were available for the all set of patients. Informed consent was obtained from each patient and the San Luigi Hospital Institutional Review Board approved the study. All samples were de-identified and

cases anonymized by a pathology staff member not involved in the study. Clinical parameters were compared and analyzed through coded data.

### ATF2 IHC analysis

To validate ATF2 expression at protein level, a cohort of 40 NSCLC samples consecutively collected (17 ADC, 17 SQC, 5 LCC and 1 BAC/AIS) was screened by immunohistochemistry.

### ATF2 and patients' CDDP therapy response

ATF2 ability to discriminate CDDP responders was tested on a retrospective cohort of 15 patients selected by extremely stringent criteria to define their response status. To have a more homogeneous cohort, only stage IIIB patients at diagnosis were selected. In addition, each patient accounted in analysis, before starting a platinum-based treatment, had Performance Status (PS) 0 but at least one disease-related symptom (i.e. cough, dyspnea and/or thoracic pain). The patients' response to CDDP therapy was evaluated using the following parameters:

### Complete Responce (CR)

Disapparence of all target and nontarget lesions was assessed as follow. Radiological CR confirmation and maintained unequivocal clinical benefit without new symptoms or signs appearance after at least 15 months or more from the first radiological and clinical response.

### Stable disease evaluation

Neither sufficient shrinkage to qualify for partial response (PR), nor sufficient increase to qualify for progressive disease (PD) (according to RECIST Criteria v.1.1) but PS and/or symptoms deterioration sufficient to require a change in therapy.

### Partial response evaluation

It is considered as PR when at least 30% decrease in the sum of diameters of target lesions, taking as reference the baseline sum diameters and persistence of one or more nontarget lesion(s) (according to RECIST Criteria v.1.1), occurs. In addition, PR patient showed symptoms resolution and benefit on global health status since starting therapy, during and after treatment. Radiological PR confirmation and maintained unequivocal clinical benefit without new symptoms or signs appearance after at least 15 months or more from the first radiological and clinical response.

### Progressive disease

Unequivocal PD in terms of both clear radiological and clinical progression with Performance Status and symptoms deterioration right at the end or during chemotherapy treatment.

### Immunohistochemistry

Formalin-fixed paraffin-embedded tissues were sliced into serial 4-μm-thick sections and collected onto charged slides for immunohistochemical (IHC) staining. After de-paraffination and rehydration through graded alcohols and phosphate-buffered saline (pH 7.4), the sections were treated in a pressure cooker for 5 min at 125°C, followed by a quick 10-second step at 90°C using EDTA buffer (pH 8.0). Sections were incubated at the optimal conditions with the following primary antibodies: (1) rabbit antibodies anti-pATF2 (1:100 dilution; 9225S, Cell Signaling Technology, Danvers, MA) and ATF2 (1:100 dilution; 9226S Cell Signaling Technology). Immunoreaction was revealed by a dextran-chain (biotin-free) detection system (MACH 1

Universal HRP-Polymer Kit with DAB, BIOCARE Medical, Concord, CA). The sections were lightly counterstained with haematoxylin. Negative control reactions were obtained by omitting the primary antibody.

The reactivity pattern was nuclear and the intensity and extent of reactivity in each case was quantified using the H-SCORE system, which ranges between 0 and 300, being the result of an intensity score from 0 to 3 multiplied by the percentage of positive tumor area (from 0 to 100%).

**Statistical analysis**

*ATF2* mRNA Cycle Threshold values (CtT) were calculated by Applied Biosystems SDS 2.1 software and normalized against the internal control *UBC* (CtR) by subtraction (CtT-CtR), generating ΔCt values. Differential *ATF2* transcript expression between ΔCt values for tumor and corresponding normal tissue samples were evaluated using t-test for paired data and expressed by the formula: $\Delta\Delta Ct = -(\Delta Ct \text{ tumor} - \Delta Ct \text{ normal})$ corresponding to $Log_2$[fold change] ($Log_2FC$). Protein and mRNA expression levels have been dichotomized into two groups of "high" and "low" expression using median value as threshold cut-off. The association between ΔΔCt and clinical-pathological variables was evaluated using the Kruskal-Wallis test. Overall survival time was calculated from the date of surgery to the death or the last follow-up date. Cox regression was used in the univariate survival analysis to determine the association of *ATF2* modulation with overall survival. Statistical analysis was performed using R statistical software.

**Results**

**NSCLC patient specimens express high level of *ATF2* at mRNA and protein level**

*ATF2* mRNA expression was measured in 86 patients with matched tumor and corresponding normal tissues obtained from surgically resected NSCLC specimens. *ATF2* mRNA was significantly upmodulated in NSCLC tumor samples compared to the paired normal specimens (Fig. 1, top left panel, $p << 0.01$, mean $Log_2(FC) = +4.7$). Current or former smoker patients had significantly higher *ATF2* mRNA levels when compared to never-smokers. Interestingly, this difference was observed in both normal and tumor tissues indicating that increased *ATF2* gene expression is most likely related to smoking exposure (Fig. 1, top right panel, Normal tissues: nonsmokers *vs*. smokers $p = 0.02$ and Tumor tissues: nonsmokers *vs*. smokers $p = 0.04$, respectively). Smoker patients expressed high ATF2 mRNA level, also in neighbor normal tissue specimens, and ATF2 upmodulation was higher when compared to nonsmokers patients specimens ($p = 0.049$, mean $Log_2FC$ 4.9 *vs*. 2.2, smokers and nonsmokers specimens, respectively). Results from IHC staining of a subset of 40 NSCLC samples consecutively collected were consistent with *ATF2* gene expression analysis. Indeed, the expression of total and phosphorylated (pATF2) ATF2 protein was higher in tumor specimens. Figure 1 shows, in two representative patients with NSCLC, different intensity of ATF2 total protein (Fig. 1 bottom panel) and phosphorylated form expression (Fig. 1 middle panel) respectively, being ATF2 protein mainly localized in the nuclear compartment of tumor cells. No further correlation was identified between ATF2 gene or protein expression and other clinical/pathological features or patients' overall survival.

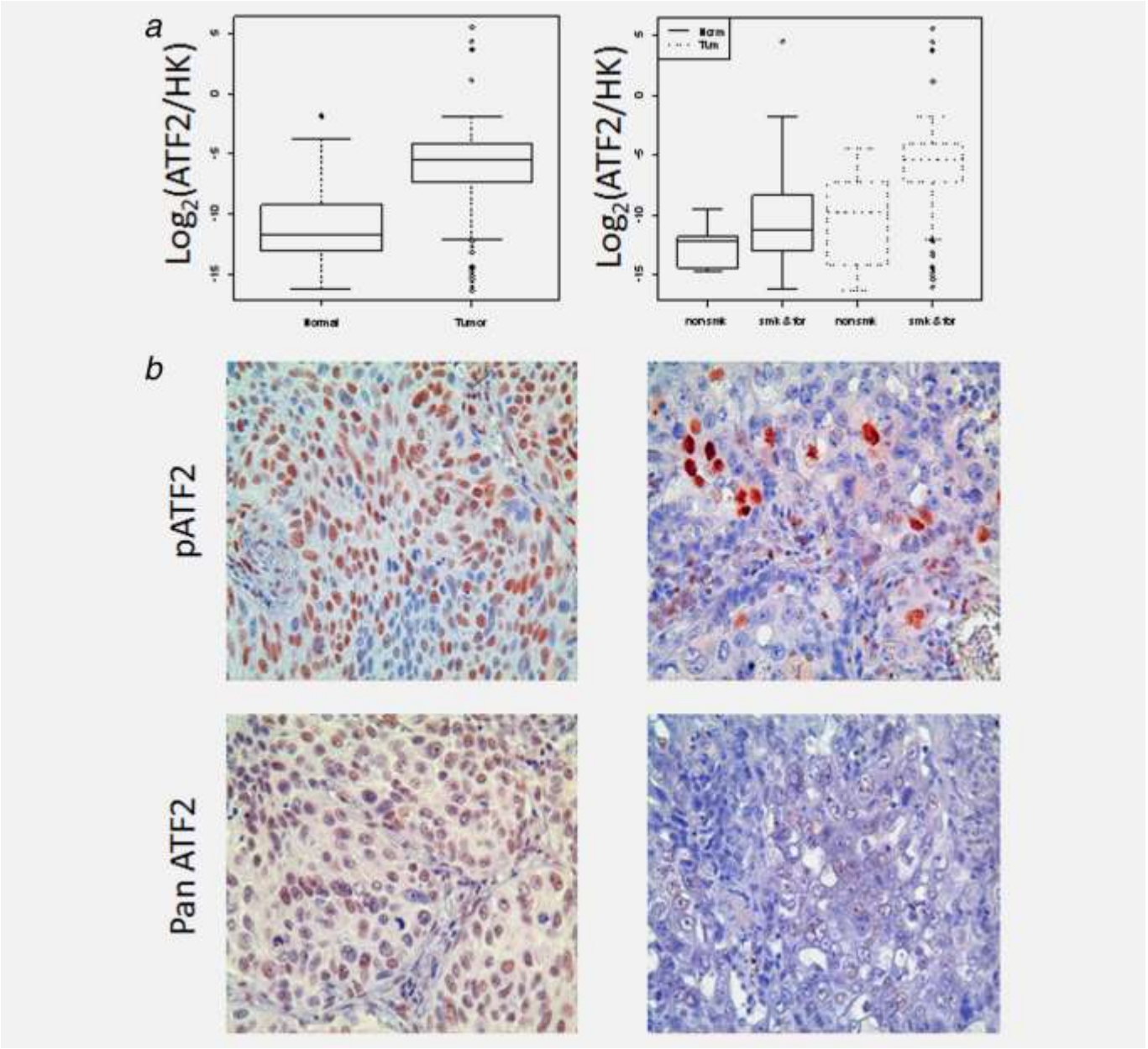


**Figure 1.**

*ATF2* expression patterns in NSCLC. A real-time PCR analysis on matched cancer and corresponding normal tissues from 86 surgically resected patients has been performed. Box plot diagram shows the increased expression level of *ATF2* mRNA in tumors respect to the paired nontumoral tissues (top left panel, $p << 0.01$, mean $Log_2(FC) = +4.7$). Current or former smoker patients expressed significantly high *ATF2* mRNA levels in both normal and tumor tissues respect to the nonsmokers samples (top right panel, $p = 0.02$ and $p = 0.04$, respectively). Norm = normal tissues, Tum = tumors, nonsmk = nonsmokers, smk and for = smokers and former smokers. Immunohistochemical staining of two NSCLCs from surgically resected specimens stained with pATF2 (middle left and right panels) and with pan ATF2 antibody (bottom left and right panels). In accord with mRNA analysis, the ATF2 and pATF2 proteins were upmodulated in NSCLC. Original magnification 200×.

**ATF2 protein expression and phosphorylation levels are increased in NSCLC cell lines resistant to CDDP**

Seven NSCLC cell lines (H522, H1395, H1299, A549, SKmes1, H596 and Calu1) were assayed for the resistance to CDDP treatment and $IC50_{24}$ calculated (see Supporting Information Table 1). $IC50_{24}$ ranged from 264 to 87 µM, being H522 and H1395 the most resistant, while H596 and Calu1 showed $IC50_{24}$ values 2–3 times lower than H522. A correlation between ATF2 protein expression (both total –ATF2- and phosphorylated –pATF2- forms) and CDDP resistance was identified (Fig. 2). In agreement with IHC data from NSCLC patients specimens (Fig. 1), CDDP treatment increased pATF2 levels mainly at the nuclear level (Fig. 3). FACS and Immunofluorescence analysis showed that the treatment with 200 µM CDDP for 6 hr enhanced pATF2 level in both H522 and H1395 resistant cell lines (Fig. 3). These results suggest that CDDP treatment represents a stress factor triggering activation, through phosphorylation, of ATF2 and, in turn, its recruitment into the nucleus of NSCLC resistant cell lines.

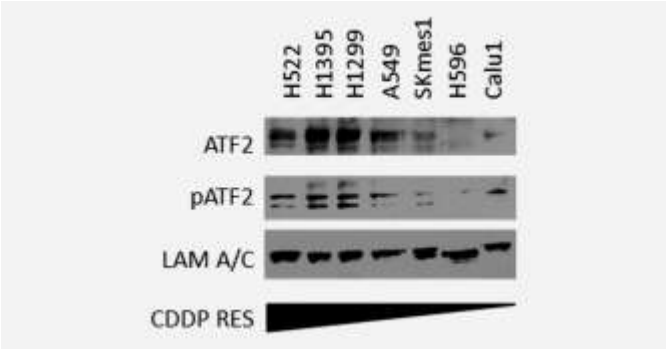


**Figure 2.**

ATF2 protein expression in cell lines correlates with its platinum resistance. Nuclear lysates obtained from indicated cell lines were subjected to Western blot analysis with pan-ATF2 and pATF2 antibody. Lamin A/C antibody was used as a loading control. Expression of inactivate and/or activate ATF2 protein correlated with platinum resistance of these cell lines obtained in MTS analysis (Supporting Information Table 1).

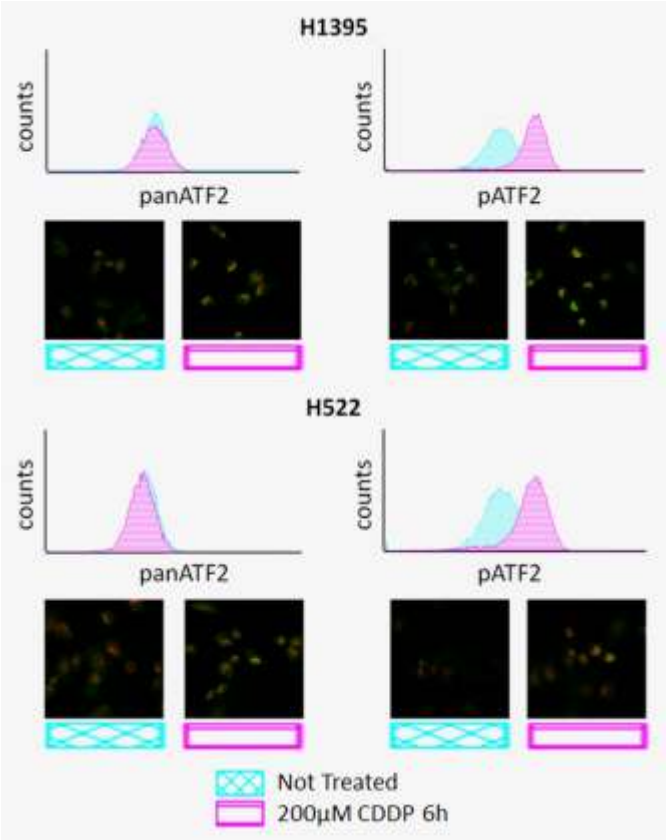

**Figure 3.**

Platinum treatment increases the phosphorylated ATF2 form and promotes its nuclear localization. FACS and immunofluorescence analyses showed that the treatment with 200-μM CDDP for 6 hr increased the expression of phosphoATF2, while did not affect the ATF2 protein levels, in both H522- and H1395-resistant cell lines. Histogram axes indicate: y = Event counts, x = Green Fluorescent in log scale. In addition, we observed nuclear localization of pATF2 protein after CDDP treatment.

**Celastrol impairs *ATF2* transcriptional activity in CDDP-resistant cell line H522 by affecting its transcription**

To functionally prove that the enriched nuclear pATF2 fraction detected in CDDP-resistant cell lines, upon CDDP treatment, was transcriptionally active, we generated 8xATF2 Responsive Elements luciferase reporter gene (8xATF2-RE-pGL3). H522 CDDP-resistant cell line was transfected with 8xATF2-RE-pGL3. After incubation of cells for 24 hr with CDDP and JNK inhibitors SP600125 or with anti-inflammatory agents (such as Celastrol and Celecoxib), ATF2 transcriptional activity was measured by luciferase reporter assay. Celastrol was the most active agent in impairing ATF2 transcriptional activity in a dose dependent manner after 2 hr of treatment (Fig. 4, top left and right panels, $p < 0.01$). Since CDDP is a backbone agent for the systemic treatment of NSCLC, we assessed the effect of both CDDP and Celastrol (alone or in combination) on ATF2 transcriptional activity. Concentration of each of single agents inferior to $IC50_{24}$ inhibited 8xATF2-RE to 70–80% of activity within 6 hr, compared to control; on the contrary, when drugs were concomitantly administered the same concentration was able to reduce the activation of 8xATF2-RE below 50% in 6 hr (Fig. 4, bottom left panel). Unexpectedly, using the exogenous DNA plasmid we did not observe of 8xATF2-RE enhanced activity after 6h platinum administration, this result could depend on experimental condition. Indeed, lipofection is slightly toxic for cell lines and could activate the stress detectors, such as ATF2, increasing ATF2-RE activity, despite CDDP absence. Thereby, in these conditions, we assessed only the signal reduction mediated by Celastrol (as well as other tested drugs). In H522 CDDP-resistant cell line, we also analyzed *ATF2* mRNA levels after removing the drugs from cell culture (recovery period). Celastrol continued to significantly down-modulate *ATF2* mRNA gene expression (Fig. 4, bottom right panel. Line 2 and 4, $Log_2(FC) = -1$, $p << 0.01$ and $p = 0.05$, respectively) and the effect was maintained for more than 12 hr after the drug wash out (Fig. 4, bottom right panel. Line 6, $Log_2(FC) = -1.56$, $p << 0.01$). Altogether, this data indicate that Celastrol was able to reduce the *ATF2* activity by reducing the production of its mRNA.

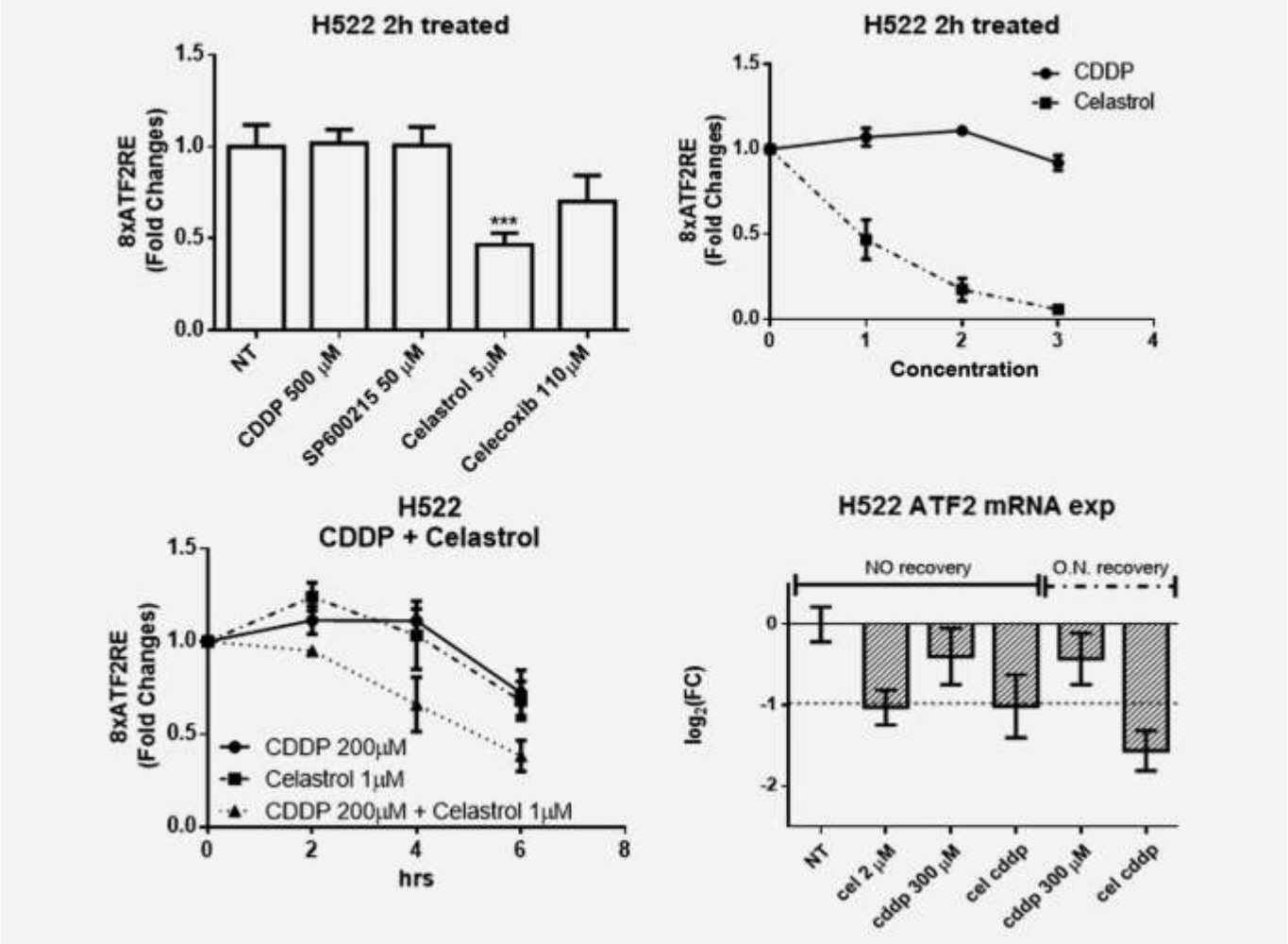


**Figure 4.**

Celastrol affects ATF2-responsive modulation and increases the effect mediated by platinum in resistant cell lines. H522 cell line was transfected with 8xATF2-RE-pGL3 using Lipofectamine 2000; after 24 hr to the transfection the cells were treated with the conditions indicated in figure and subsequentially lisated by passive lysis buffer. We tested the ability of CDDP, JNK inhibitor SP600215 and inflammation inhibitor (Celastrol and Celecoxib) to affect *ATF2*-mediated modulation. Celastrol was able to reduce significantly *ATF2*-mediated modulation of *ATF2*-responsive element after 2 hr of 5-μM treatment ($p < 0.01$, top left panel). In addition, this effect was directly proportional to concentration of Celastrol utilized in the experiment (top right panel). A similar result was identified evaluating effect of interaction between CDDP and Celastrol on 8xATF2-RE promoter activation. Sub $IC50_{24}$ concentration of single drugs inhibits 8xATF2-RE at 70–80% in 6 hr compared to not treated cell line; in contrast, the same concentration of drugs mix was able to reduce the activation of 8xATF2 under 50% in 6 hr (bottom left panel). Celastrol significantly downmodulates ATF2 mRNA gene expression (bottom right panel, Lines 2 and 4, $Log_2(FC) = -1$, $p << 0.01$ and $p = 0.05$, respectively) and its effect was maintained even after the drug was washed out and let cells recovery overnight (bottom right panel, Line 6, $Log_2(FC) = -1.56$, $p << 0.01$).

**Celastrol resensitizes to chemotherapy CDDP-resistant cell lines expressing high level of ATF2**

To evaluate the hypothesis that Celastrol may resensitize cell lines to CDDP, we performed a viability assay to assess whether Celastrol-induced ATF2 inhibition could contribute to revert CDDP resistance. As indicated in Table 1, Celastrol and CDDP showed mainly additive effect on

cell lines viability. On the contrary, in CDDP-resistant cells expressing high ATF2 levels, a synergic interaction between CDDP and Celastrol was observed (H1395 +24% and H522 +57% in comparison to each drug administered alone). A similar pattern of inhibition was detected also when Gemcitabine, a commonly used drug for NSCLC chemotherapy, was tested (Supporting Information Table 2). Differently from what observed with CDDP, in the experiment with Gemcitabine the CI index showed an additive effect in the CDDP-resistant cell lines. These data indicate that Celastrol-enhanced sensibilization of cells to Gemcitabine. In particular, in the H1395 cell line the Gemcitabine $IC50_{24}$ decreased from 190 µM, when used alone, to 0.84 µM when used in combination with Celastrol. Similarly, in H522 cell line Gemcitabine $IC50_{24}$ dropped from 452 to 4 µM when combined with Celastrol. The Gemcitabine $IC50_{24}$ in the presence of CDDP were 3.47 µM and 4.6 µM for H1395 and H522 cell lines, respectively. Gemcitabine/CDDP $IC50_{24}$ values are higher than those obtained when Gemcitabine was combined with Celastrol. In both cell lines, the presence of CDDP or Gemcitabine did not reduce the Celastrol $IC50_{24}$ (Table 1 or Supporting Information Table 3). This "absence of effect" on Celastrol $IC50_{24}$ turns to a weaken correlation index, without affecting the original hypothesis, which supports the potential efficacy of Celastrol (in combination or before standard therapy) to increase the response to CDDP-based chemotherapy.

Table 1. Celastrol/CDDP correlation index

| | **$IC50_{24}$ mix (µM)** | | |
|---|---|---|---|
| **Cell lines** | **Celastrol** | **CDDP** | **Correlation index** |
| 1. Cells were cultured for 24 hr with different drug concentrations, each administered alone or in combination of each concentration, and then cells viability was assessed by the MTS colorimetric assay. IC50 values were calculated by evaluating the viability data with sigmoidal dose response analysis using GraphPad software and Combination Index (CI) calculated using mutually nonexclusive formula (see Material and Methods). | | | |
| H522 | 0.80 | 15.49 | 0.43 |
| H1395 | 1.34 | 26.24 | 0.86 |
| H1299 | 1.11 | 21.58 | 0.95 |
| A549 | 2.17 | 42.95 | 1.29 |
| SKmes1 | 1.82 | 35.56 | 0.92 |
| H596 | 0.96 | 18.28 | 0.65 |
| Calu1 | 1.05 | 20.23 | 0.94 |

**Celastrol inhibits *cJUN* expression**

*ATF2* is a member of AP1 transcription factor family, which can act as either hetero- or homo-dimers. A known partner of *ATF2* is *cJUN*, whose gene expression is associated with drug resistance. To test which mechanism is involved in NSCLC resistant cell lines, we analyzed *cJUN* gene expression, at both mRNA and protein level, by incubating the H522 cell line with Celastrol and CDDP for 15 hr at $IC50_{24}$ x1 and $IC50_{24}$ x2. In these conditions, CDDP highly increased expression and activation of *cJUN*, both at protein and mRNA level (Fig. 5). Conversely, Celastrol

increased only *cJUN* mRNA but at levels not even comparable to those reported upon CDDP treatment (Fig. 5, top left panel). The combination of the two agents produced effects comparable to those of Celastrol alone. Surprisingly, the effect of CDDP treatment was not restricted to the expression of *cJUN* itself, most likely affecting its post-transcriptional modification status. Indeed, we observed a cJUN doublet following CDDP treatment (Fig. 5, top right panel, line 2) resembling the hyper-phosphorylated cJUN band previously reported by Gou.[32] To test the hypothesis that CDDP leads to cJUN hyper-phosphorylation, we incubated CDDP treated H522 cell line lysates with Calf Intestinal Alkaline Phosphatase (CIAP). The treatment with CIAP reduced the intensity of the band with higher molecular weight indicating that this was likely due to cJUN phosphorylation (Fig. 5, bottom left panel, line 5 and 6 and bottom right panel). Furthermore, we observed that Celastrol was able to impair this process (Fig. 5, top right panel, line 4 and 5 and bottom left panel, line 4).

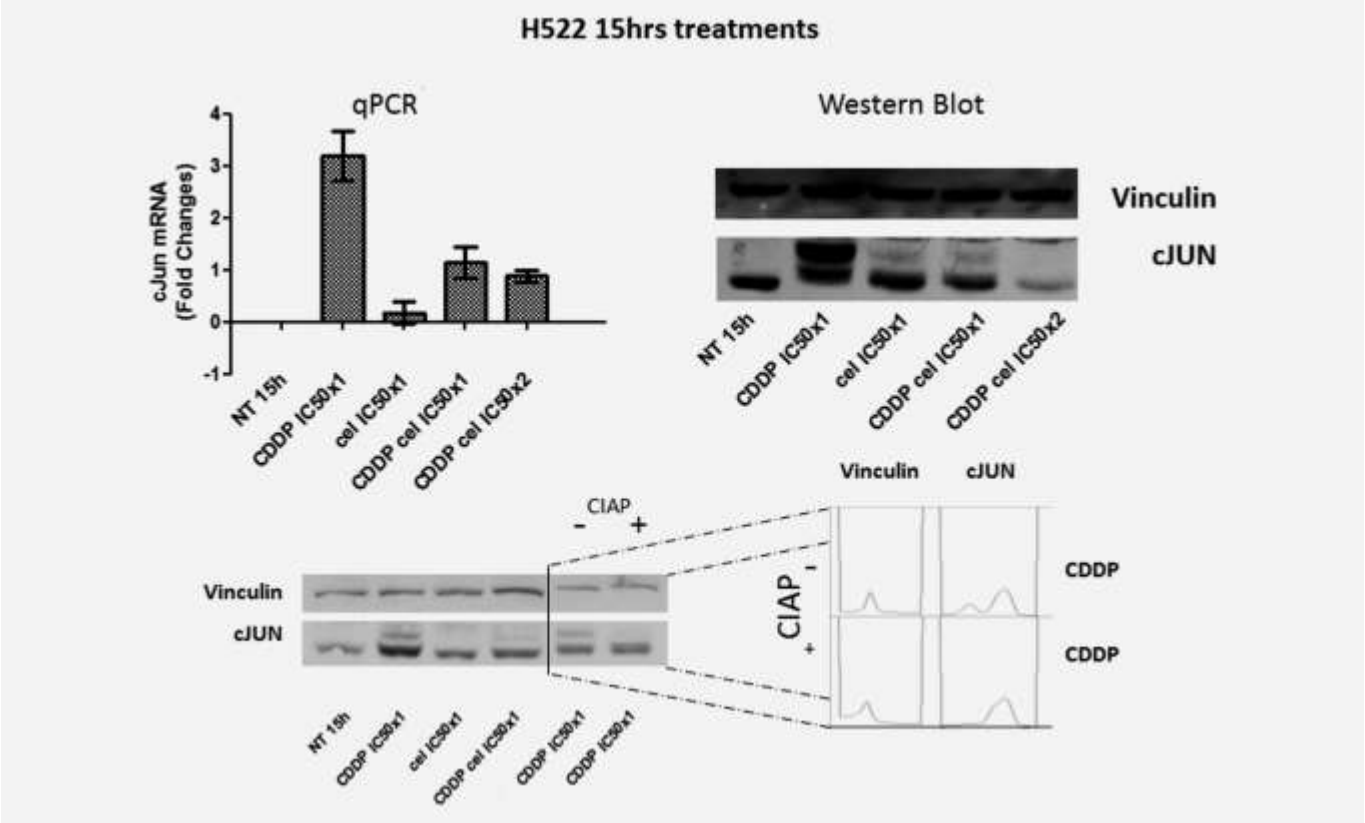


**Figure 5.**

Celastrol blocks cJUN hyperphosphorylation and its regulation at both mRNA and protein level. H522 cell line was treated for 15 hr with several drugs conditions; *cJUN* mRNA and protein levels were evaluated. Platinum significantly upmodulate *cJUN* mRNA (up left panel. Line 2, $Log_2$(FC) >3) and protein levels (up right panel, Line 2). The treatment with 10u of CIAP enzyme for 3 hr clearly reduces the intensity of band with high molecular weight observed upon platinum response (bottom left panel, Lines 5 and 6). Bands quantification performed with ImageJ software highlighted such effect. The analysis identified only a peak in cJUN CIAP-treated sample respect to not CIAP-treated ones (bottom right panel). On this basis, Celastrol was able to block cJUN hyperphosphorylation (top right panel, Lines 2 and 4; bottom left panel, Lines 2 and 4).

**Celastrol inhibits the expression of several genes involved with CDDP resistance**

In our study, we observed that Celastrol was able to affect *ATF2* and *cJUN* expression at both protein and mRNA levels. ATF2/cJUN dimerization controls key cellular processes and their deregulation was reported in several tumors, often associated with drug resistance. Based on this

assumption, to gain further insights on the pathways affected by Celastrol, we analyzed in H522 cell line the expression of a panel of genes involved in CDDP resistance and/or implicated in central biological processes. Fifteen hours of treatment with 2 μM of Celastrol drastically inhibited several genes involved in DNA repair (*ATM1, BRCA1, BRCA2, ERCC1, XPA, TOP2A*), proliferation (*PARP1, AURKA, E2F1, RRM1, RRM2*), stress response and DNA replication (*ATF7B, POLH, ZNF143*) (Supporting Information Table 3. All $p < 0.01$ after Bonferroni correction).

**ATF2 protein activation correlates with worse outcome in CDDP-treated advanced NSCLC patients**

Data obtained from the present study supports the hypothesis of *ATF2* deregulation in NSCLC specimens, but because tumor samples were obtained from a surgical series not exposed to chemotherapy, it is not possible to verify the association between *ATF2* gene expression and sensitivity to CDDP. Therefore, we further tested ATF2 protein by IHC in a restricted cohort of patients with advanced NSCLC treated with CDDP-based chemotherapy (Supporting Information Table 4, n=15). We focus this preliminary analysis on ATF2 ability to discriminate CDDP responders and, for this reason, we selected patients with extremely stringent criteria to define their response state, as specified in the section material and methods. The data indicated a correlation between H-Score of pATF2 and CDDP resistance (grouping together patients with an objective response vs. those with disease stabilization or progression during chemotherapy) (unpaired Mann-Whitney $p = 0.022$; PD/stable disease median H-Score=125; PR/CR median H-Score=25).

**Discussion**

Platinum-based chemotherapy, in combination with Gemcitabine, docetaxel, paclitaxel or pemetrexed (limited to nonsquamous NSCLC), represents the standard of care for nonselected patients with advanced NSCLC. However, systemic treatment fails in most of the patients because NSCLC shows rapid emergence of acquired resistance to platinum-based chemotherapy,[4] thus prompting several attempts to address which molecular mechanisms are underlying CDDP resistance with the aim to increase the efficacy (i.e. *ERCC1* and *RRM1* expression levels are used as therapy response predictors).

*ATF2* is a member of the helix-loop-helix b-ZIP transcription factor family, often associated to chemo- and radio-resistance.[8, 33] Agents that inhibit *ATF2* activate, both *in vitro* and *in vivo*, apoptotic pathways leading to an increased response to radio- and chemo-therapy.[34] In the present study, we reported a correlation between ATF2 protein expression, as total and phosphorylated form, and CDDP resistance (Fig. 2 and Supporting Information Table 1). Furthermore, we identified that treatment of cell lines with CDDP increases phosphoATF2 levels, and its recruitment to nuclear compartment of H522 and H1395 CDDP-resistant cell lines (Fig. 3). This data are in agreement with a previous study reporting a correlation between *ATF2* expression and the resistance to CDDP treatment in breast carcinoma BT474 cell line.[8] In details, Shah *et al*. identified the same nuclear punctiform pattern shown in Figure 2 and concluded that such peculiar staining could indicate ATF2 localization in DNA repair foci following DNA damage.[35]

Our results indicate that Celastrol, an active triterpene extracted by the Chinese herb "Thunder of God Vine", down-modulates ATF2-mediated transcription in a dose dependent manner (Fig. 4). Pharmacological inhibition of *ATF2* by Celastrol was able to restore platinum response in CDDP-resistant cell lines expressing high level of ATF2 protein (Supporting Information Table 1). Moreover, we detected a synergistic effect between CDDP and Celastrol in H522 and H1395 cell lines, two cell lines expressing the highest ATF2 protein levels (Fig. 2). Quite likely, these results may be related to the Celastrol ability to suppress *ATF2* mRNA expression, since its effect was already detectable shortly after initial treatment (2 hr) and maintained for 24 hr after drug removal (Fig. 4 bottom right panel). Additionally, in both tested cell lines we observed that Celastrol increased the efficacy of Gemcitabine (Gem) in association with CDDP, a doublet chemotherapy

commonly used for the systemic treatment of NSCLC. The effect of the combination of Gem and Celastrol was enhanced compared to that of Gem/CDDP. This data is in agreement with previous studies in which it was demonstrated that Celastrol synergistically enhances the cytotoxicity of radiotherapy and chemotherapy.[22-24]

Similarly, to all members of its family, *ATF2* needs to undergo homo- or heterodimerization to mediate its biological effect. This interaction is finely tuned by several stimuli and it is responsible for different cellular response ranging from apoptosis to proliferation.[7, 9, 36] One of the crucial partners of this dimeric complex is the proto-oncogene *cJUN*. The JNK/c-Jun/ATF2 pathway regulates a plethora of target genes containing AP1-binding sites, including those that controlling survival and apoptosis, metalloproteinases and nuclear hormone receptors. Deregulation of these processes could leads to drug resistance.[37, 38] The protective role of *cJUN* against cisplatin cytotoxicity was reported in a series of studies involving modified cell lines expressing dominant negative cJUN form (dnJUN). By contrast, the expression of dnJUN resulted in enhanced sensitivity to a panel of DNA-damaging agents with different mechanisms of action, including UV-C, doxorubicin, daunorubicin, methionine-S-methyl sulfonium chloride (MMS), actinomycin D and etoposide.[39] Moreover, *ATF2* may regulate *cJUN* transcript expression and often ATF2 inhibitors act interfering with the formation of cJUN/ATF2 heterodimers.[34, 40] We observed an increased *cJUN* expression in response to incubation of cell lines with CDDP at both transcriptional and protein level. The CDDP mediated *cJUN* production/activation led to cJUN hyperphoshorylation as observed in Figure 5 similarly to data previously reported by Gou *et al*.[32] Conversely, Celastrol down-modulated *cJUN* impairing cJUN hyperphoshorylation (Fig. 5). Our results suggest that the decrease of cJUN phosphorylation combined with *ATF2* down modulation, observed in response to Celastrol, contributes to restoring cellular CDDP sensitivity. In line with this hypothesis, Bhoumik *et al*. identified that an *ATF2* peptide inhibitor causes alteration in AP1 dimers, leading to spontaneous apoptosis in melanoma cells.[34]

ATF2/cJUN dimerization has been reported in several tumors being often associated to drug resistance. cJUN/ATF2 complex activity is responsible for Bcl-xL activation and stimulates cell proliferation.[41] A relationship between cJUN/ATF2 complex and growth factors independent cellular proliferation in chick embryo fibroblasts has been reported.[9] It has been observed that *ATF2* affects the transcription of around 180 genes following treatment with CDDP and mostly the genes were activated via ATF2/cJUN complex.[36] As a follow up investigation, Celastrol was added for 15 hr to the CDDP-resistant cell line H522; it has been shown that Celastrol inhibits the expression of some genes involved in DNA repair, proliferation and platinum resistance (Supporting Information Table 3). More interestingly, Celastrol inhibited the transcription of genes such *ERCC1* and *RRM1* often associated with platinum and Gemcitabine resistance, respectively (Supporting Information Table 3). However, Celastrol modulated also other genes such as *BRCA1*, *BRCA2*, *AURKA* and *POLH*, which have been previously identified as de-regulated in NSCLC patients.[42-44] In particular, we previously reported a correlation between *AURKA* mRNA expression and tumor differentiation grade in NSCLC.[44] In addition, *POLH* expression levels were strongly associated with shorter patient survival in platinum-treated patients.[43] The results prompted us to hypothesize that Celastrol could be useful *in vivo* to down-modulate the expression of these genes thus restoring the response to chemotherapeutic agents.

At the clinical level, we have investigated *ATF2* gene expression in 86 matched cancer and corresponding normal tissues from surgically resected NSCLC patients. *ATF2* mRNA was significantly upmodulated in NSCLC tumor samples when compared to corresponding normal counterpart (Fig. 1, top left panel). Current or former smoker patients had significantly higher *ATF2* mRNA levels when compared to never-smokers, both in tumoral and in normal tissue specimens (Fig. 1, top right panel). Interestingly, it has been reported that in mouse bone marrow derived dendritic cells, cigarette smoke extract increased the phosphorylation of c-jun, c-fos and ATF2, sustaining the chronic airway inflammation characterizing the chronic obstructive pulmonary disease.[45] In rat vascular smooth muscle cells, acrolein, a major component of cigarette smoke,

causes stimulation of multiple members of the MAPK family, mediating cJUN and ATF2 activation.[46] In rat cerebral arteries, lipid-soluble cigarette smoke particles induced phosphorylation of ATF-2 and Elk-1 which in turn are responsible for the enhanced expression of both extracellular-matrix-related gene MMP13 and vascular AT1 receptors.[47] Our results on normal tissue derived by smokers were in line with these previous reports, supporting the hypothesis that ATF2 is upmodulated and activated in response to smoke stress. IHC staining for ATF2 revealed its prevalent nuclear localization in NSCLC specimens (Fig. 1), a finding also observed in cell lines CDDP-treated (Fig. 3) and clinically associated with poor prognosis in melanoma.[10] This increased level of ATF2 expression in lung tissues could contribute to a microenvironment status, favoring the development of the resistance to chemotherapy through the cJUN/ATF2 pathway. Several studies indicate that drugs used in lung cancer chemotherapy, such as CDDP and Taxanes, act through MAPK kinases and JNK/cJUN pathways to mediated apoptosis.[48, 49] Based on our data, it can be speculated that if chemotherapeutic agents activate JNK/cJUN pathway, leading to higher ATF2 levels, this in NSCLC could trigger resistance mechanisms throughout the ATF2/cJUN complex. According to this hypothesis, we have identified a correlation between pATF2 expression levels and clinical response to platinum-based chemotherapy. In particular, our preliminary analysis suggests that pATF2 could discriminate responding to nonresponding patients (Supporting Information Table 4). Given the small patient number satisfying our stringent criteria recruited for this analysis, further studies are needed to evaluate if the inhibition of *ATF2* activity mediated by Celastrol or other specific inhibitors will increase the patients response to therapy as we here identified in CDDP-resistant cell lines.

In conclusion, the study revealed that in NSCLC cell lines a correlation between ATF2 protein expression and CDDP resistance occurred. Furthermore, our results suggest the possibility to increase CDDP response by inhibiting ATF2/cJUN function by Celastrol. It is the observation that NSCLC specimens display high ATF2 protein levels localized into the nucleus as it occurred in the CDDP-resistant cell lines. Therefore, we propose that these patients could benefit by a treatment aiming to reduce the activity of ATF2 protein thus leading to an increase CDDP response. Further studies in this direction will be necessary to create the basis for personalized target therapy in lung cancer, with the target to maximize the benefit of therapy and reducing the collateral effect and drug resistance.